

# The structures of *m*-benzyne and tetrafluoro-*m*-benzyne

Christopher E. Smith and T. Daniel Crawford<sup>a)</sup>  
*Department of Chemistry, Virginia Tech, Blacksburg, Virginia 24061*

Dieter Cremer  
*Department of Physics and Department of Chemistry, University of the Pacific, 3601 Pacific Avenue,  
Stockton, California 95211-0110*

(Received 10 January 2005; accepted 17 February 2005; published online 3 May 2005)

The structures of *m*-benzyne and its fluorinated derivative, tetrafluoro-*m*-benzyne, were investigated using coupled cluster methods including triple excitations [CCSD(T) and CCSDT], different reference wave functions (spin-restricted Hartree–Fock, spin-unrestricted Hartree–Fock, and Brueckner), and different basis sets [6-31G(*d,p*) and correlation-consistent valence triple-zeta (cc-pVTZ)]. The inclusion of triple excitations in conjunction with *d*- and *f*-type polarization functions is paramount to correctly describe through-bond delocalization of the monocyclic form. At the highest level of theory, the C1–C3 distance of the minimum energy form of *m*-benzyne is 2.0 Å and the profile of the potential energy surface along the C1–C3 distance is that of an asymmetric, single well, in agreement with previous density-functional theory and coupled cluster studies. In addition, the calculated CCSD(T) fundamental frequencies are in excellent agreement with the measured infrared frequencies, thus confirming the monocyclic form of *m*-benzyne. For tetrafluoro-*m*-benzyne, however, the increased eclipsing strain between the ring-external C–X bonds stabilizes the bicyclo[3.1.0]hexatriene form: the C1–C3 distance is calculated at the CCSD(T)/cc-pVTZ level to be approximately 1.75 Å, which is in the range of elongated CC bonds. Computed harmonic vibrational frequencies compare reasonably well with the experimental neon-matrix difference spectrum and provide further evidence for the existence of a bicyclic form. © 2005 American Institute of Physics. [DOI: 10.1063/1.1888570]

## I. INTRODUCTION

1,3-Didehydrobenzene (commonly known as *m*-benzyne, see Fig. 1) and its derivatives provide excellent examples of the often symbiotic relationship between theory and experiment. *m*-Benzynes are stable only at low temperatures and can be characterized by matrix isolation infrared spectroscopy,<sup>1–7</sup> and quantum chemical calculations can reproduce the measured spectrum provided they also correctly describe the molecule's geometry and electronic structure.<sup>1,8–16</sup> Hence, agreement between measured and calculated infrared spectra is synonymous with identification and structural characterization. Although this strategy of combining theory and experiment promises useful insight into the electronic structure of labile compounds not amenable to other structural investigations, it is easily hampered by complicating factors that may make the comparison problematic. These may have to do with the experimental conditions (e.g., low resolution of the measured spectra, limited detection range, presence of other molecules in the matrix, etc.) or the limitations of the theoretical description (e.g., multireference effects, basis set incompleteness, etc.). (For a recent review of many of the issues hampering theoretical descriptions of benzyne diradicals, see Ref. 17.)

Marquardt, Sander, and Kraka carried out the photolytic destruction of [2,2]*meta*-paracyclophane-2,9-dione trapped in an argon matrix at 10 K and hypothesized that *m*-benzyne

was one of the products.<sup>1</sup> Theoretical calculations using coupled cluster theory supported this conclusion: the coupled cluster singles and doubles method with perturbative triples [CCSD(T)] (Ref. 18) and the 6-31G(*d,p*) basis set<sup>19</sup> predicts a monocyclic structure (structure 1 of Fig. 1) whose harmonic vibrational spectrum shows good agreement with the experimental infrared difference spectrum.<sup>1</sup> Kraka and Cremer, using the same level of theory, predicted a C1–C3 bond length of ca. 2.0 Å and a relatively weak biradical character of just 20%.<sup>8,9</sup> These investigations were later repeated by generating *m*-benzyne from other precursors, and in each case the same infrared spectrum was observed.<sup>4</sup>

Several authors have also performed density-functional theory (DFT) (Ref. 20) and wave-function-based calculations to explore the potential energy surface (PES) along the *m*-benzyne C1–C3 distance.<sup>12,13</sup> At smaller values of *r*(C1–C3) a second structure, bicyclo[3.1.0]hexatriene (structure 2 of Fig. 1) may be located, which, despite its high ring strain resulting from the existence of a cyclopropenyl unit and two inverted carbon atoms (C1 and C3), is remarkably stable relative to the open form. However, whether the monocyclic or bicyclic structure is most stable depends heavily on the type of method used, and the choice of density functional, wave function, basis set, correlation correction, etc. can have a dramatic effect on the shape of the PES.<sup>12,13</sup> Among density functionals, in particular, the restricted three-parameter exchange functional of Becke plus the correlation functional of Lee, Yang, and Parr (RB3LYP) functional<sup>21,22</sup>

<sup>a)</sup>Electronic mail: crawdad@vt.edu

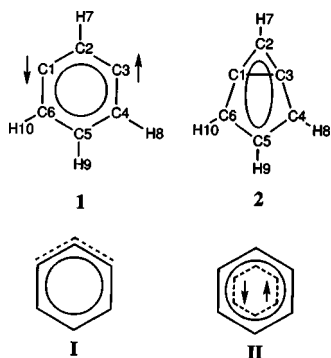


FIG. 1. Possible structural forms of *m*-benzyne: a monocyclic singlet biradical (1) vs a bicyclic closed-shell singlet (2); the  $\sigma$ -allylic structure of Winkler and Sander (Ref. 13) (I) vs a  $\sigma$ -delocalized structure (II). In structure 2, the ring denotes the  $\pi$  system, which remains essentially intact (relative to benzene) after the formation of the C1–C3 bond. In structure I, the dotted line indicates the presence of  $\sigma$ -through-bond coupling between C1–C3 and C1–C2/C2–C3. For structure II, the circle indicates the delocalized  $\pi$  system, the dashed hexagon through-bond delocalization, and the coupled arrows a strong degree of spin coupling leaving little, but still finite biradical character.

predicts the bicyclic structure to be the most stable, whereas the RBLYP functional<sup>22,23</sup> prefers the monocyclic structure, and an extensive discussion exists in the literature over the most appropriate choice of method for biradicals.<sup>12,24–31</sup>

Wenk and Sander recently reported the generation of tetrafluoro-*m*-benzyne in solid neon at 3 K identified by its corresponding infrared difference spectrum.<sup>5,6</sup> Just as for the parent *m*-benzyne, density functional calculations give widely varying results depending on the choice of functional. Based upon their previous studies of *m*-benzyne, Wenk and Sander concluded that the RB3LYP functional overestimates the interaction between the radical centers. They therefore preferred the RBLYP functional, which predicts a monocyclic structure.

However, Hess has recently disputed the conclusions of these investigations,<sup>14</sup> and has suggested that still higher levels of theory should be applied to finally lay to rest the question of *m*-benzyne's structure. Indeed, the variability of computed results from coupled cluster theory with respect to the choice reference determinant, an important aspect for related compounds such as 1,4-didehydrobenzene (also known as *p*-benzyne),<sup>32</sup> has not yet been examined for *m*-benzyne or tetrafluoro-*m*-benzyne. Furthermore, calculated infrared spectra have been exclusively based on the harmonic approximation combined with various scaling procedures to simulate the true fundamental infrared vibrational frequencies of the compound.<sup>1,4,10,12</sup> Although this approach is common in quantum chemistry,<sup>33</sup> it makes spectra comparison more a qualitative rather than the needed quantitative exercise.

Several other questions must be answered in connection with the *m*-benzyne (and tetrafluoro-*m*-benzyne) problem: (1) What level of theory is required to obtain the most reliable description of the two *m*-benzyne forms, or, equivalently, how can one obtain a reliable description of the PES along the C1–C3 distance? (2) What is the shape of this PES profile: a double well, a simple single well, a strongly asymmetric single well, or a broad, flat single-well embedding

both *m*-benzyne forms and leading to a large amplitude vibration? (3) Can one assess the answers to these two questions via a comparison of measured and calculated infrared vibrational spectra of *m*-benzyne?

Some of these questions have been investigated in the past. For example, the most extensive study of *m*-benzyne to date is that of Winkler and Sander,<sup>13</sup> who used both DFT and wave-function-based methods to investigate the PES along the C1–C3 distance. They found that pure functionals based on the generalized gradient approximation (GGA) such as BLYP were superior to hybrid functionals such as B3LYP for *m*-benzyne because they produced energy profiles that more closely mimicked those from higher level coupled cluster theory. However, Kraka, Cremer, and co-workers have shown that this is due to the fact that BLYP includes nonspecific, nondynamical correlation effects via the semilocal exchange functional.<sup>24–26,28–31</sup> In this way the stability of the restricted BLYP solution is artificially increased and an unrestricted BLYP solution suppressed so that zero biradical character is enforced for any *m*-benzyne form. B3LYP, which contains only a reduced amount of nondynamical electron correlation, has an unrestricted solution in the case of *m*-benzyne that is higher in energy than the restricted solution for the bicyclic form.

Standard DFT with the approximate exchange-correlation functionals in use today fails to describe the multiconfigurational character of *m*-benzyne. The use of BLYP and other GGA functionals in a sense disguises the true problem by predicting a perfect coupling of the single electrons (via peripheral delocalization or an unlikely long CC bond close to 2 Å). Accordingly, the reactivity of a typical closed shell system rather than a molecule with some biradical character is predicted. More reliable results can only be obtained if a two-configurational approach such as the restricted ensemble Kohn–Sham approach is used with a hybrid functional to exclude at least partly the nondynamic correlation introduced through the exchange functional.<sup>31</sup> But even a two-configurational DFT approach has to be verified with a method that works without any assumptions and approximations and is known to provide reliable results in the case of biradicals. Clearly coupled cluster is such a method.

The objective of the present work is to reconsider the ability of various single-determinant-reference coupled cluster methods<sup>34,35</sup> in the prediction of the structure of *m*-benzyne and tetrafluoro-*m*-benzyne. We have examined the influence of the reference molecular orbitals (spin-restricted, spin-unrestricted, or Brueckner) on the predicted structure, as well as basis-set effects and higher levels of dynamic electron correlation. We have computed energy profiles of both molecules using structural optimizations at coupled cluster levels of theory with varying basis sets. In addition, we have considered the potential importance of anharmonicity on the vibrational spectrum of *m*-benzyne by computing the fundamental vibrational transition wave numbers. These results provide, among other things, reliable reference data for comparison to more approximate methods, such as DFT.

TABLE I. Optimized geometrical parameters of *m*-benzynes (bond distances in angstroms, angles in degrees, and energies in  $E_h$ ).

	6-31G( <i>d,p</i> )						cc-pVTZ		
	CCSD			CCSD(T)			CCSDT	CCSD	CCSD(T)
	RHF	UHF	Brueckner	RHF	UHF	Brueckner	RHF	RHF	RHF
$r(C_1-C_3)$	1.563	1.563	1.561	2.106	2.088	2.105	2.093	1.551	2.026
$r(C_2-C_3)$	1.351	1.351	1.351	1.377	1.372	1.377	1.376	1.343	1.364
$r(C_3-C_4)$	1.384	1.384	1.384	1.383	1.379	1.383	1.384	1.376	1.372
$r(C_4-C_5)$	1.411	1.411	1.411	1.405	1.401	1.405	1.406	1.404	1.398
$r(C_2-H)$	1.080	1.080	1.080	1.078	1.078	1.078	1.079	1.074	1.072
$r(C_4-H)$	1.077	1.077	1.077	1.082	1.082	1.082	1.083	1.071	1.076
$r(C_5-H)$	1.083	1.083	1.083	1.086	1.086	1.086	1.087	1.078	1.080
$\theta(C_1-C_2-C_3)$	70.7	70.7	70.6	99.8	99.1	99.7	99.0	70.5	95.9
$\theta(C_3-C_4-C_5)$	107.7	107.7	107.7	117.3	117.0	117.3	117.1	107.7	116.7
$\theta(C_4-C_5-C_6)$	111.9	111.9	111.9	114.5	114.5	114.5	114.3	111.7	113.4
$\theta(C_3-C_4-H)$	126.3	126.3	126.3	120.5	120.6	120.6	120.6	126.3	120.7
Energy	-230.221 066	-230.221 066	-230.219 548	-230.268 076	-230.266 229	-230.268 097	-230.237 040	-230.490 523	-230.550 092

## II. COMPUTATIONAL APPROACH

We have investigated the structures of *m*-benzynes and tetrafluoro-*m*-benzynes at the CCSD,<sup>36,37</sup> CCSD(T),<sup>18,38</sup> and full CCSDT levels of theory.<sup>39,40</sup> In order to identify potential problems associated with the underlying molecular orbital definitions, we utilized three types of reference determinants with the CC methods: spin-restricted Hartree–Fock (RHF), spin-unrestricted Hartree–Fock (UHF), and Brueckner orbitals.<sup>41,42</sup> Two basis sets were used in this study: the Pople-type split-valence 6-31G(*d,p*) basis set,<sup>19</sup> and the larger correlation-consistent valence triple-zeta basis set (cc-pVTZ) developed by Dunning,<sup>43</sup> which corresponds to a  $(10s5p2d1f/5s2p1d)/[4s3p2d1f/3s2p1d]$  basis.

Optimized geometries were obtained using analytic energy gradients at the CCSD and CCSD(T) levels of theory with the RHF (Refs. 44–47) and UHF (Ref. 48) reference determinants, as well as at the CCD level with Brueckner orbitals.<sup>42</sup> Finite differences of energies were used to obtain gradients at the full CCSDT and B-CCD(T) levels. Energy profiles of *m*-benzynes and tetrafluoro-*m*-benzynes were obtained from optimized structures with constrained C1–C3 distances.

Harmonic vibrational frequencies were determined using analytic energy second derivatives at the CCSD and CCSD(T) levels of theory with the RHF and UHF reference functions,<sup>49–51</sup> numerical differentiation of analytic gradients at the B-CCD level,<sup>42</sup> and numerical differentiation of energies at the B-CCD(T) level. Infrared absorption intensities were computed for all methods for which at least analytic energy gradients were available. RHF-CCSD(T) fundamental vibrational frequencies of *m*-benzynes were determined using second-order vibrational perturbation theory with cubic and semidiagonal quartic force constants computed via finite differences of analytic second derivatives using the method described by Stanton, Lopreore, and Gauss.<sup>52</sup>

$T_1$  and  $T_2$  excitation amplitudes were monitored as diagnostics of the quality of the coupled cluster wave functions. All electrons were correlated at the CCSD and CCSD(T)

levels of theory, and the 1s core electrons on carbon and fluorine were frozen at the full CCSDT level. All calculations were performed using the ACESII program system.<sup>53</sup>

## III. RESULTS AND DISCUSSION: *M*-BENZYNE

Table I summarizes coupled cluster predictions of the structure of *m*-benzynes. With the CCSD/6-31G(*d,p*) method, all three reference determinants—RHF, UHF, and Brueckner—predict a bicyclic structure as the global minimum on the PES, with a C1–C3 distance of 1.56 Å. (At this geometry, there is no true UHF wave function, i.e., the RHF determinant is stable to spin-symmetry breaking. Thus, the RHF-CCSD and UHF-CCSD structures given in Table I are identical.) However, triple excitations produce a dramatic change in *m*-benzynes's predicted structure: the CCSD(T)/6-31G(*d,p*) level of theory predicts a monocyclic structure as the global minimum, with C1–C3 distances of 2.11, 2.09, and 2.11 Å, respectively, with the RHF, UHF, and Brueckner reference determinants. This qualitative difference continues at the full RHF-CCSDT level of theory, which gives a C1–C3 distance of 2.09 Å. We observed similar trends using the larger cc-pVTZ basis set, as reported for the RHF-CCSD and RHF-CCSD(T) levels of theory in Table I. If we consider the fact that the larger cc-pVTZ basis set reduces the C1–C3 distance by 0.08 Å, we predict that a value of ca. 2.013 Å would be obtained at the CCSDT/cc-pVTZ level of theory.

### A. Electronic structure of *m*-Benzynes

Figure 2(a) presents the RHF-CCSD and RHF-CCSD(T) energy profiles of *m*-benzynes (relative to the minimum at the given level of theory) as a function of the C1–C3 distance, where all other geometrical parameters were optimized. These diagrams illustrate clearly the difference in predicted structures, with the CCSD minimum at 1.56 Å and the CCSD(T) minimum at 2.11 Å, and with a noticeable “shoulder” on both profiles.

CCSD provides an accurate account of pair correlation in the singles and double space, and it should therefore correctly describe the degree of through-space pairing between

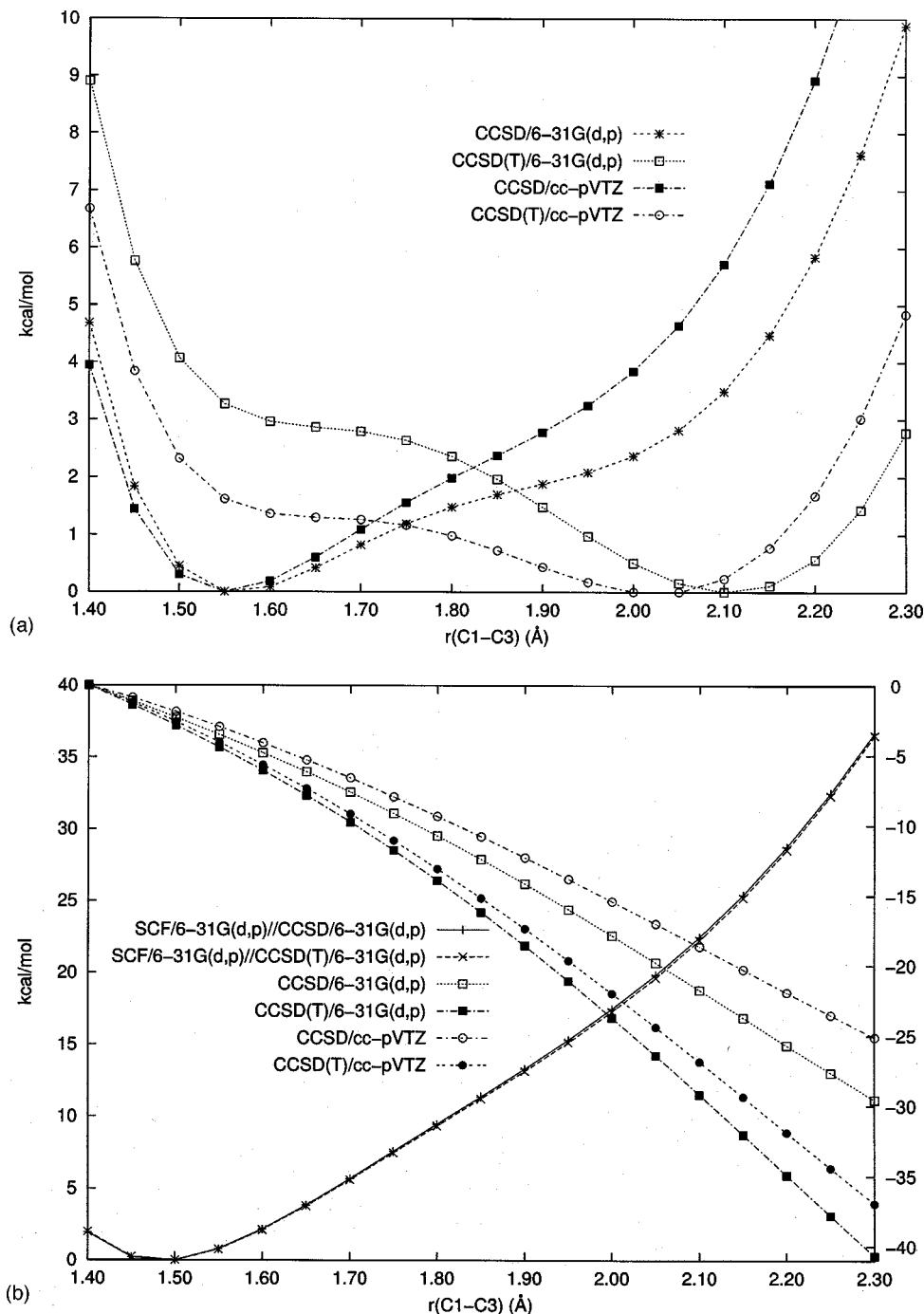


FIG. 2. RHF-CCSD and RHF-CCSD(T) C1-C3 energy profiles for *m*-benzyne using a 6-31G(*d,p*) basis set. Structural parameters were optimized for fixed C1-C3 distances. Energies are reported relative to the global minimum on the respective PES. (a) Total energies; (b) RHF energies (left-hand y axis) and change in correlation energy with respect to the C1-C3 distance, relative to the correlation energy at  $r(\text{C1-C3})=1.40$  Å (right-hand y axis).

the single electrons at C1 and C3. However, it includes only disconnected three-electron correlation effects so that through-bond interactions of the single electrons are underestimated.<sup>54,55</sup> Accordingly, it exaggerates the importance of forming a C1-C3 bond and wrongly predicts the existence of a bicyclic form. Both basis sets used [6-31G(*d,p*) and cc-pVTZ] predict an asymmetric PES with a shoulder at the position of the open form. The larger basis set stabilizes the bicyclic form stronger relative to the open form (4–5 kcal/mol higher in energy) than the smaller basis set (2–3 kcal/mol).

CCSD(T), on the other hand, gives a more balanced account of both pairwise and connected three-electron correlation effects so that the stabilization of the open form by

through-bond delocalization is correctly assessed. This is confirmed by Fig. 2(b), which gives the self-consistent field (RHF) (left-hand y axis) and correlation contributions (right-hand y axis) to the total energies. We note that the RHF energy profiles are identical, indicating that the differing shapes of the CCSD and CCSD(T) surfaces are due entirely to electron correlation effects. The shapes of the CCSD and CCSD(T) correlation energy curves in Fig. 2(b) are similar, but the steeper slope of the latter leads to a shift in the minimum to a larger C1-C3 distance shown in the total energy profile given in Fig. 2(a). There is also a clear change in the CCSD(T) PES when using the larger cc-pVTZ basis set. The shoulder at the position of the bicyclic form is lowered significantly from 3.2 to 1.6 kcal/mol, which leads to a shift of

the minimum from 2.11 to 2.05 Å [Fig. 2(a)]. Clearly, the correct PES profile along the C1–C3 distance corresponds to an asymmetric, single-minimum potential. This result is confirmed by UHF- and Brueckner-CCSD(T) calculations that do not significantly change the shape of the PES profile.

## B. Biradical character of *m*-benzynes

What is the biradical character of the reference wave function in the two most important regions of the energy profiles described above—the bicyclic region for which CCSD predicts a minimum and the monocyclic region preferred by CCSD(T)? One measurement of such multireference character is the size of the  $T_2$  cluster amplitudes. For short C1–C3 distances, the maximum  $T_2$  RHF-CCSD amplitude is 0.09. (As noted earlier, UHF-CCSD gives identical results in this case because the RHF wave function is spin-stable.) For longer C1–C3 distances, on the other hand, the maximum RHF-CCSD  $T_2$  amplitude increases to 0.24 [to a double excitation from the highest occupied molecular orbital (HOMO) to the lowest unoccupied molecular orbital (LUMO)] clearly indicating greater biradical character in the reference function. (UHF-CCSD gives nearly identical values.) As a second measure of biradical character in the wave function, we have also computed natural orbital occupation numbers (NOON). For the RHF-CCSD wave function in the short C1–C3 region (i.e., the bicyclic structure), the HOMO and LUMO NOON values are 1.92 and 0.07, respectively, while in the long C1–C3 region (i.e., the monocyclic structure) the values are 1.75 and 0.24, in agreement with the results obtained by Kraka and Cremer.<sup>8,9</sup> Again, we see that the biradical character increases with the C1–C3 distance, as expected, though, its magnitude is significantly smaller than for *p*-benzynes, with HOMO and LUMO NOON values of 1.18 and 0.82, respectively.<sup>32</sup>

We note also that Winkler and Sander<sup>12</sup> concluded via a natural bond-orbital analysis that *m*-benzynes's monocyclic structure should not be described as a biradical but rather as a  $\sigma$ -allylic structure (Fig. 1, structure I) referring to the fact that the two single electrons can delocalize from the  $a_1$ -symmetrical C1–C3 bonding orbital into the antibonding C2–H7 orbital. The same authors show, however, that this delocalization effect is much stronger in the case of the bicyclic compound and that significant contributions arise from the through-bond interactions involving  $\sigma$ -bonds C1–C2, C2–C3, C4–C5, and C5–C6. Hence, structure II of Fig. 1 may provide a more realistic description of the electronic situation, which is characterized by increased pairing of the single electrons caused by their delocalization through the whole  $\sigma$  framework of the ring. Representation II is also to be preferred as it illustrates explicitly the partial biradical character and does not conflict with the fact that a partial allene structure (formula I) should cause a widening of the C1–C2–C3 angle (relative to benzene), where the opposite is actually the case.

The reduced biradical character of *m*-benzynes is the reason that the molecule has a relatively low tendency to abstract hydrogen atoms.<sup>56</sup> Instead it undergoes reactions with nucleophiles, which of course does not imply a preference

for the bicyclic versus the monocyclic form, because a monocyclic structure with delocalized single electrons is easily polarizable and can react either as an electrophile or as a nucleophile.

## C. The infrared spectrum of *m*-benzynes

Marquardt *et al.* reported *m*-benzynes's infrared (IR) difference spectrum from the isolated photolytic decomposition of [2,2]*meta*-paracyclophane-2,9-dione in solid argon at 10 K.<sup>1,3</sup> Table II includes experimental IR vibrational data reported by Sander, and theoretical vibrational frequencies determined by CCSD/ and CCSD(T)/6-31G(*d,p*). The latter are in agreement with those given by Marquardt *et al.*<sup>1,4</sup> Among the totally symmetric modes, only three directly affect the C1–C3 distance:  $\omega_1$  (C1–C2–C3 bending),  $\omega_2$  (out-of-phase breathing of C1–C2–C3 and C4–C5–C6), and  $\omega_5$  (C1–C2/C3–C2 symmetric stretching). However, only  $\omega_5$  is computed to have any significant intensity. Again we find that for both CCSD and CCSD(T) methods the computed IR frequencies are invariant with respect to choice of reference determinant. This is in contrast to *p*-benzynes for which Crawford *et al.* found that the RHF reference wave function suffered from MO instabilities, leading to dramatic shifts in the computed vibrational frequencies.<sup>32</sup> Figures 3(a) and 3(b) are comparisons of the experimental IR vibrational spectrum vs those determined by theory in the 500–1600  $\text{cm}^{-1}$  range. The CCSD spectrum shown in Fig. 3(a) includes nine absorption peaks within this range, three of which cannot be matched to any of the peaks in the experimental difference spectrum. Furthermore, the CCSD  $b_1$  vibrational mode at 1093  $\text{cm}^{-1}$  does not reasonably fit with any of the experimental absorption peaks.

The CCSD(T) infrared spectrum [Fig. 3(b)], on the other hand, accounts for all the experimental absorption peaks within this range and correctly reproduces the relative intensities as well. Due to the somewhat anharmonic nature of the PES (*vide supra*), we also calculated CCSD(T) fundamental frequencies as reported in Table III. Most of the shifts are small (less than 50  $\text{cm}^{-1}$ ) and most are negative, except for the 545, 743, and 818  $\text{cm}^{-1}$  harmonic frequencies, which lie slightly below the corresponding experimental fundamentals at 547, 751, and 824  $\text{cm}^{-1}$ , respectively. In nearly every case, the computed fundamentals align superbly with the experimental infrared absorption peaks, as illustrated in Fig. 3(b). Thus, based on the above evidence, we agree with Marquardt *et al.*,<sup>1</sup> Kraka *et al.*,<sup>12</sup> and Sander *et al.*<sup>4</sup> that the infrared spectrum clearly identifies the monocyclic structure of *m*-benzynes.

## IV. RESULTS AND DISCUSSION: TETRAFLUORO-*M*-BENZYNES

Table IV summarizes coupled cluster predictions of the structure of tetrafluoro-*m*-benzynes. At the CCSD/6-31G(*d,p*) level of theory, all three reference functions predict a nominally bicyclic structure, with C1–C3 distances (in angstroms) of 1.621 (RHF), 1.600 (UHF), and 1.617 (Brueckner), though we note that (1) the agreement among the orbital choices is significantly poorer for  $\text{C}_6\text{F}_4$  than for

TABLE II. Computed harmonic vibrational frequencies (in  $\text{cm}^{-1}$ ) for *m*-benzynes determined using the 6-31G(*d,p*) basis set. Normalized infrared absorption intensities (in  $\text{km/mol}$ ) are given in parentheses.

	CCSD			CCSD(T)			Argon, 10 K <sup>a</sup>
	RHF	UHF	Bruceckner	RHF	UHF	Bruceckner	
$\omega_1(a_1)$	522.3(0.76)	522.3(0.76)	533.3(0.76)	386.4(0.05)	371.7(0.07)	389.7	
$\omega_2(a_1)$	839.9(0.00)	839.9(0.00)	840.8(0.00)	848.7(0.01)	849.1(0.01)	849.6	
$\omega_3(a_1)$	1094.0(0.00)	1094.0(0.00)	1095.6(0.00)	1051.8(0.00)	1078.7(0.01)	1055.0	
$\omega_4(a_1)$	1115.8(0.00)	1115.8(0.00)	1117.6(0.00)	1118.4(0.00)	1130.6(0.01)	1115.4	
$\omega_5(a_1)$	1466.2(0.14)	1466.2(0.14)	1468.4(0.14)	1454.2(0.14)	1471.8(0.16)	1451.5	1402(0.15)
$\omega_6(a_1)$	1882.2(0.03)	1882.2(0.03)	1885.9(0.03)	1706.6(0.01)	1757.3(0.03)	1707.5	
$\omega_7(a_1)$	3247.0(0.22)	3247.0(0.22)	3249.4(0.21)	3210.1(0.22)	3201.1(0.24)	3201.8	3037(0.05)
$\omega_8(a_1)$	3270.7(0.16)	3270.7(0.16)	3272.1(0.15)	3255.5(0.07)	3258.0(0.07)	3270.7	
$\omega_9(a_1)$	3306.2(0.11)	3306.2(0.11)	3308.0(0.11)	3289.2(0.05)	3289.3(0.05)	3296.8	
$\omega_{10}(a_2)$	611.4(0.00)	611.4(0.00)	612.0(0.00)	496.6(0.00)	517.4(0.00)	494.8	
$\omega_{11}(a_2)$	808.5(0.00)	808.6(0.00)	809.4(0.00)	824.6(0.00)	843.0(0.00)	826.2	
$\omega_{12}(b_1)$	576.4(1.00)	576.4(1.00)	577.7(1.00)	544.5(1.00)	553.5(1.00)	549.9	547(1.00)
$\omega_{13}(b_1)$	923.9(0.02)	923.9(0.02)	925.4(0.02)	974.8(0.28)	986.7(0.30)	982.7	936(0.25)
$\omega_{14}(b_1)$	1093.3(0.28)	1093.3(0.28)	1094.3(0.28)	1151.6(0.00)	1152.8(0.00)	1139.2	
$\omega_{15}(b_1)$	1201.0(0.00)	1201.0(0.00)	1202.0(0.00)	1284.4(0.00)	1285.5(0.01)	1273.8	
$\omega_{16}(b_1)$	1335.7(0.17)	1335.7(0.17)	1337.1(0.17)	1336.3(0.00)	1331.8(0.00)	1298.0	
$\omega_{17}(b_1)$	1390.6(0.24)	1390.6(0.24)	1392.0(0.24)	1419.9(0.00)	1412.9(0.00)	1420.8	
$\omega_{18}(b_1)$	1606.8(0.18)	1606.8(0.18)	1609.7(0.18)	1543.9(0.18)	1578.5(0.14)	1537.1	1486(0.15)
$\omega_{19}(b_1)$	3301.8(0.20)	3301.8(0.20)	3303.6(0.20)	3250.5(0.12)	3253.2(0.12)	3241.0	
$\omega_{20}(b_2)$	297.4(0.15)	297.4(0.15)	297.3(0.15)	366.6(0.04)	379.3(0.04)	366.7	
$\omega_{21}(b_2)$	564.3(0.00)	564.3(0.00)	564.3(0.00)	478.7(0.03)	509.4(0.04)	482.6	
$\omega_{22}(b_2)$	779.8(0.28)	779.8(0.28)	781.8(0.28)	743.5(0.54)	766.3(0.60)	743.7	751(0.45)
$\omega_{23}(b_2)$	811.0(0.61)	811.0(0.61)	811.7(0.60)	818.2(0.10)	837.4(0.12)	820.3	824(0.20)
$\omega_{24}(b_2)$	973.0(0.01)	973.0(0.01)	973.3(0.01)	917.7(0.00)	951.5(0.00)	917.8	

<sup>a</sup>Reference 1.

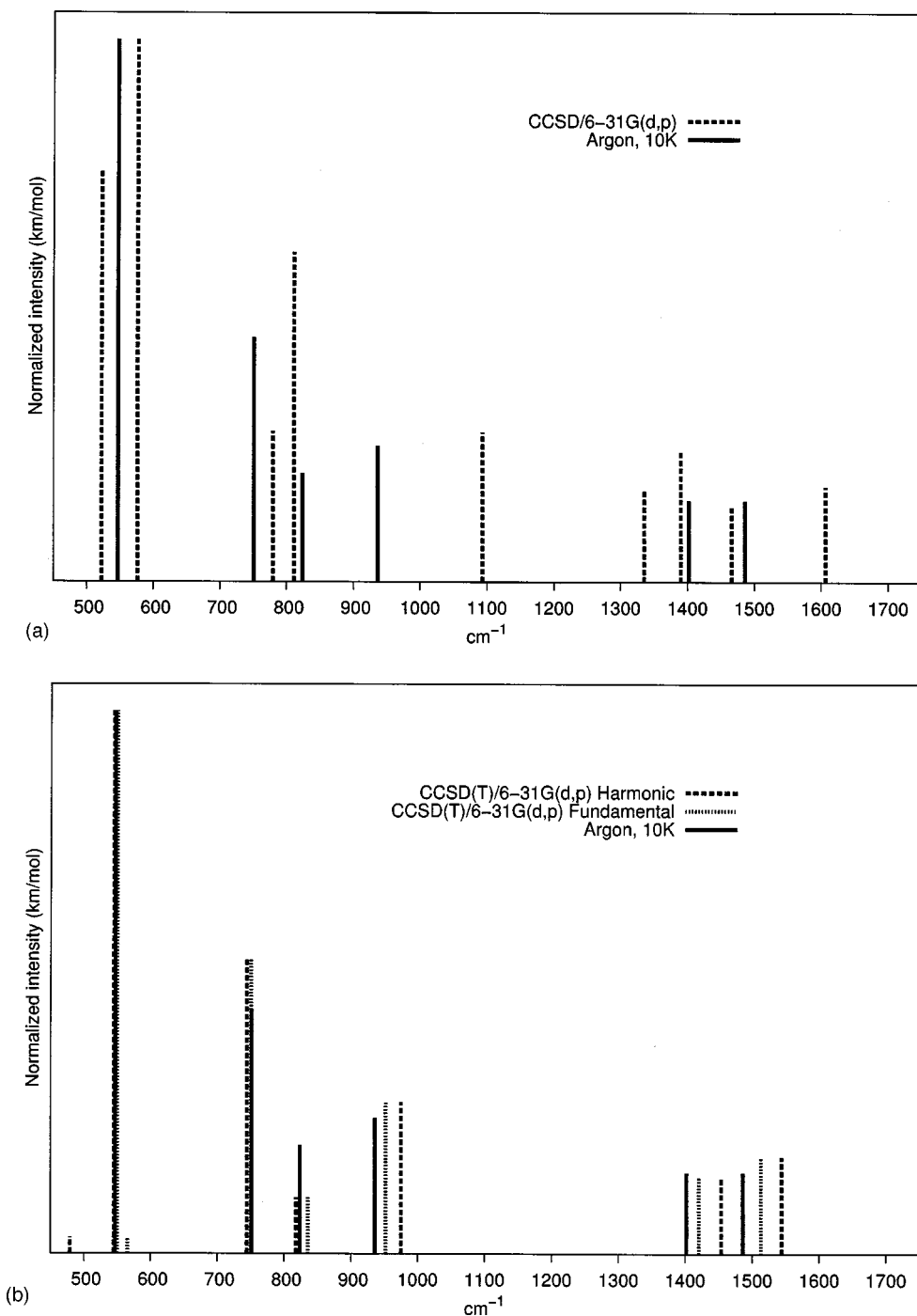


FIG. 3. RHF-CCSD and CCSD(T) infrared vibrational spectra for *m*-benzyne using a 6-31G(*d,p*) basis. The experimental infrared difference spectrum reported by Marquardt *et al.* (Ref. 1) is compared to (a) the CCSD harmonic infrared spectrum and (b) the CCSD(T) harmonic and fundamental infrared spectra.

*m*-benzyne and (2) the C1–C3 distance in C<sub>6</sub>F<sub>4</sub> is 0.04–0.05 Å longer than in *m*-benzyne (cf. Table I). Again, triple excitations lead to a widening in the C1–C3 distance, ranging from 0.08–0.12 Å, depending on the choice of reference, but much smaller than that observed for *m*-benzyne, for which the C1–C3 distance shifts by more than 0.5 Å between CCSD and CCSD(T).

Clearly, the steric repulsion of the substituents F8, F9, and F10 is sufficient to overcome all electronic factors that favor a C1–C3 distance of 2 Å or larger. Indeed, it is likely that this distance would be even shorter if the substituent F7 at C2 did not destabilize the C1–C3 interactions. We rationalize these results as follows: (a) The inductive effect of fluorine withdraws electron density out of the C1–C3 region

into the  $\sigma^*(\text{C2-F7})$  orbital; (b) At the same time, the in-plane lone pair of F7 can donate density into the C1–C3 antibonding orbital, thus hindering the formation of a shorter C1–C3 bond; (c) The  $\pi$ -donor capacity of F7 also stabilizes the bicyclic structure because it supports a resonance structure in which the  $\pi$  system of the *m*-benzyne splits into an aromatic allyl anion unit and a nonaromatic (as opposed to antiaromatic) cyclopropenyl cation. (We also note that the  $\pi$ -donor effects of F8, F9, and F10 serve to somewhat offset the effect of F7 and destabilize the bicyclic form.)

Figure 4 presents RHF-CCSD/ and RHF-CCSD(T)/6-31G(*d,p*) energy profiles of tetrafluoro-*m*-benzyne (relative to the minimum-energy structure at each level of theory) as a

TABLE III. Anharmonicities and fundamental vibrational frequencies ( $\text{cm}^{-1}$ ) of *m*-benzynes computed at the RHF-CCSD(T)/6-31G(*d,p*) level of theory.

	Anharmonicity	Fundamental	Argon, 10 K <sup>a</sup>
$\omega_1(a_1)$	-20.3	366.1	
$\omega_2(a_1)$	0.9	849.6	
$\omega_3(a_1)$	-9.3	1042.5	
$\omega_4(a_1)$	-21.8	1096.5	
$\omega_5(a_1)$	-33.6	1420.6	1402 (0.15)
$\omega_6(a_1)$	-46.5	1660.1	
$\omega_7(a_1)$	-133.3	3076.9	3037 (0.05)
$\omega_8(a_1)$	-138.2	3117.3	
$\omega_9(a_1)$	-146.1	3143.0	
$\omega_{10}(a_2)$	1.9	498.5	
$\omega_{11}(a_2)$	5.2	829.8	
$\omega_{12}(b_1)$	5.5	550.0	547 (1.00)
$\omega_{13}(b_1)$	-22.8	951.9	936 (0.25)
$\omega_{14}(b_1)$	-24.6	1127.1	
$\omega_{15}(b_1)$	-19.8	1264.6	
$\omega_{16}(b_1)$	-37.3	1299.0	
$\omega_{17}(b_1)$	-40.5	1379.4	
$\omega_{18}(b_1)$	-30.9	1513.0	1486 (0.15)
$\omega_{19}(b_1)$	-155.1	3095.5	
$\omega_{20}(b_2)$	0.6	367.1	
$\omega_{21}(b_2)$	86.8	565.6	
$\omega_{22}(b_2)$	6.9	750.4	751 (0.45)
$\omega_{23}(b_2)$	17.9	836.0	824 (0.20)
$\omega_{24}(b_2)$	32.9	950.6	

<sup>a</sup>Reference 1.

function of the C1–C3 distance, where all geometrical parameters were optimized. As for *m*-benzynes [cf. Fig. 2(a)], the CCSD level clearly favors the bicyclic structure with only a slight shoulder as the C1–C3 distance increases. However, the CCSD(T) level produces a very flat PES, with a minuscule barrier of only 0.07 kcal/mol separating the inner minimum at C1–C3=1.744 Å and an outer minimum at C1–C3=1.981 Å, similar to that found for *m*-benzynes. Although this result could support the hypothesis that the true structure is characterized by a large amplitude vibration en-

compassing open and bicyclic forms as extreme cases, the 6-31G(*d,p*) basis is clearly too small to provide an accurate description. The shape of the PES is significantly basis-set dependent, as shown in Fig. 4, which also plots RHF-CCSD(T)/cc-pVTZ energies computed at the same RHF-CCSD(T)/6-31G(*d,p*) constrained structures. With the larger basis set, the outer minimum disappears, leaving only a single minimum with a C1–C3 distance at approximately 1.75 Å, comparable to the RHF-CCSD(T) inner minimum with the 6-31G(*d,p*) basis set. Clearly, the minimum energy structure of tetrafluoro-*m*-benzynes corresponds more to that of a bicyclo[3.1.0]hexatriene than to that of a monocyclic structure considering the fact that C–C distances of 1.75 Å should still provide some weak bonding. In addition, we note that this distance is significantly shorter than that given by BLYP/6-311++G(*d,p*) (1.909 Å).<sup>5</sup>

### A. The infrared spectrum of tetrafluoro-*m*-benzynes

Wenk and Sander used UV photolysis of 1,3-diiodo-2,4,5,6-tetrafluorobenzene in solid neon at 3 K and recorded an infrared difference spectrum that they subsequently assigned to tetrafluoro-*m*-benzynes based in part on DFT calculations.<sup>5,6</sup> Table V compares the experimental results of Wenk and Sander to the CCSD/ and CCSD(T)/6-31G(*d,p*) harmonic vibrational frequencies associated with the optimized structures given in Table IV. Among the totally symmetric modes,  $\omega_1$  (C1–C2–C3 bending),  $\omega_4$  (ring breathing), and  $\omega_5$  (C1–C2/C3–C2 symmetric stretching) directly affect the C1–C3 distance, but only  $\omega_5$  is computed to have significant intensity. (It is also worth noting that the relative intensity of  $\omega_5$  is significantly higher than in the parent *m*-benzynes, for which the mode has a similar C–C stretching structure.) The computed infrared frequencies vary little with respect to the choice of reference determinant (at most 50  $\text{cm}^{-1}$ ), though the variation is somewhat larger than for *m*-benzynes. Figures 5(a)–5(c) are comparisons of the experimental IR vibrational spectrum vs those determined by

TABLE IV. Optimized geometrical parameters of tetrafluoro-*m*-benzynes (bond distances in angstroms, angles in degrees, and energies in  $E_h$ ) computed with the 6-31G(*d,p*) basis set.

	CCSD			CCSD(T)			CCSD(T) <sup>a</sup>
	RHF	UHF	Brueckner	RHF	UHF	Brueckner	RHF
$r(\text{C}_1\text{--C}_3)$	1.621	1.600	1.617	1.744	1.680	1.753	1.981
$r(\text{C}_2\text{--C}_3)$	1.344	1.334	1.335	1.338	1.337	1.339	1.348
$r(\text{C}_3\text{--C}_4)$	1.367	1.364	1.368	1.370	1.367	1.371	1.375
$r(\text{C}_4\text{--C}_5)$	1.404	1.400	1.405	1.405	1.403	1.406	1.401
$r(\text{C}_2\text{--F})$	1.317	1.317	1.318	1.325	1.324	1.326	1.330
$r(\text{C}_4\text{--F})$	1.341	1.342	1.342	1.344	1.345	1.345	1.344
$r(\text{C}_5\text{--F})$	1.329	1.329	1.330	1.333	1.332	1.334	1.336
$\theta(\text{C}_1\text{--C}_2\text{--C}_3)$	74.8	74.8	74.6	81.3	77.9	81.8	94.5
$\theta(\text{C}_3\text{--C}_4\text{--C}_5)$	109.1	109.1	109.0	111.6	110.2	111.8	115.7
$\theta(\text{C}_4\text{--C}_5\text{--C}_6)$	111.8	111.8	111.8	112.0	112.1	112.1	113.5
$\theta(\text{C}_3\text{--C}_4\text{--F})$	127.0	127.3	127.1	125.3	126.2	125.2	122.7
Energy	-626.231 418	-626.230 941	-626.192 360	-626.290 841	-626.289 857	-626.292 003	-626.290 948

<sup>a</sup>“Outer” minimum-energy structure described in the text.

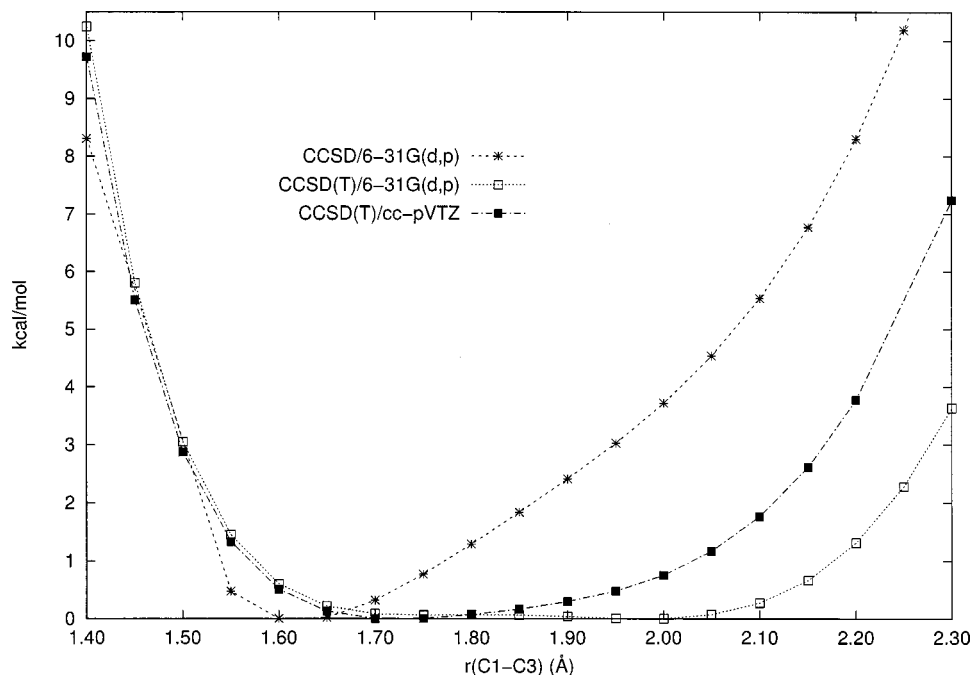


FIG. 4. RHF-CCSD and RHF-CCSD(T) C1-C3 energy profiles for tetrafluoro-*m*-benzyne using the 6-31G(*d,p*) and cc-pVTZ basis sets. Structural parameters were optimized for fixed C1-C3 distances at the RHF-CCSD(T)/6-31G(*d,p*) level of theory. Energies are reported relative to the global minimum on the respective PES.

theory in the 400–2100  $\text{cm}^{-1}$  range for the RHF-CCSD, inner-RHF-CCSD(T), and outer-RHF-CCSD(T) structures, respectively.

The CCSD frequencies compare reasonably well, except for one additional low-frequency line in the 400–700  $\text{cm}^{-1}$  range and two low-intensity lines between 1200 and 1400  $\text{cm}^{-1}$ . In addition, the intensity of the line at 2031  $\text{cm}^{-1}$  is much too large, assuming it should compare to the experimental line at 1818  $\text{cm}^{-1}$ . The CCSD(T) data compare somewhat better with experiment, apart from the low-intensity line at 1443  $\text{cm}^{-1}$  for the inner minimum [Fig. 5(b)] and a missing low-frequency, low-intensity line near 500  $\text{cm}^{-1}$  for the outer minimum [Fig. 5(c)]. The highest-frequency line compares better to experiment in position for both sets of CCSD(T) data, but are too high in intensity, just as for CCSD.

If one considers the substantial basis-set dependence of the structures in Table IV and the CCSD(T) energy profile in Fig. 4, as well as the need for anharmonicity corrections in the high-frequency range (cf. Table III for the parent molecule), then the accuracy of the CCSD(T)/6-31G(*d,p*) level of theory cannot be considered the final authority on the structure of tetrafluoro-*m*-benzyne. Indeed, additional CCSD(T)/cc-pVTZ data, which were not feasible in the present work due to computational limitations, will be necessary to finally resolve this issue. However, there are three reasons that suggest that the experimental spectrum supports a bicyclic rather than monocyclic form.

(1) For the CCSD(T) spectrum calculated at C1-C3 = 1.744 Å all measured infrared bands can be assigned. It is more than likely that the “extra” low-intensity lines suggested by theory cannot be resolved in the experimental spectrum. In addition, the infrared band at 1500  $\text{cm}^{-1}$  [which is missing in the CCSD(T) spectrum calculated for C1-C3 = 1.981 Å] *must* belong to the difference infrared spectrum of tetrafluoro-*m*-benzyne.

(2) Basis set and anharmonicity corrections are often simulated by using a scaling factor of 0.96 for CCSD(T)/6-31G(*d,p*) frequencies,<sup>1,10</sup> a particularly useful technique in the high-frequency range to approach experimental values from above. In the case of the CCSD(T) spectrum calculated for C1-C3 = 1.744 Å this would lead to an improvement between theory and experiment for the bands between 1500 and 1830  $\text{cm}^{-1}$ , but not in the case of the CCSD(T) spectrum calculated for C1-C3 = 1.981 Å.

(3) For the bicyclic structure, the band  $\omega_5$ , which is the only totally symmetric band that leads to a reduction of the C1-C3 distance, is one of the most intense transitions according to CCSD(T) calculations at C1-C3 = 1.744 Å, but is significantly reduced in intensity at C1-C3 = 1.981 Å. In the experimental spectrum this is indeed the most intense band (cf. Table V).

We conclude that the infrared spectrum does indeed suggest a bicyclic structure with a relatively long C1-C3 bond of approximately 1.75 Å. It is beyond the computational possibilities presently available to determine if measured infrared spectrum confirms a large amplitude vibration involving  $\omega_5$ .

## B. Biradical character of tetrafluoro-*m*-benzyne

The biradical character of the tetrafluoro-*m*-benzyne structures, as estimated by the magnitudes of the  $T_1$  and  $T_2$  cluster amplitudes, is rather small. For the CCSD/6-31G(*d,p*) structure  $T_1(\text{max})=0.03$  and  $T_2(\text{max})=0.08$ . (UHF-CCSD gives a similar maximum  $T_2$ , and a somewhat larger maximum  $T_1$  of 0.08.) For the RHF-CCSD(T)/6-31G(*d,p*) structure with C1-C3 = 1.75 Å, these values are similar:  $T_1(\text{max})=0.03$  and  $T_2(\text{max})=0.11$ . The HOMO and LUMO NOON values for each structure are comparable: CCSD = 1.92/0.07, CCSD(T) = 1.89/0.09. Hence, tetrafluoro-*m*-benzyne is best described as a bicyclic structure with an elongated C1-C3 bond.

TABLE V. Computed harmonic vibrational frequencies (in  $\text{cm}^{-1}$ ) for tetrafluoro-*m*-benzynes determined using the 6-31G(*d,p*) basis set. Normalized infrared absorption intensities (in  $\text{km/mol}$ ) are given in parentheses.

	CCSD			CCSD(T)			CCSD(T) <sup>a</sup>			Neon, 3 K <sup>b</sup>
	RHF	UHF	Brueckner	RHF	UHF	RHF	RHF	UHF	RHF	
$\omega_1(a_1)$	288.1(0.00)	289.6(0.00)	289.9(0.00)	124.7(0.00)	241.8(0.04)	151.9(0.01)				
$\omega_2(a_1)$	439.5(0.09)	467.1(0.09)	447.9(0.09)	307.2(0.02)	323.3(0.05)	316.6(0.01)				
$\omega_3(a_1)$	530.5(0.01)	530.6(0.01)	531.1(0.01)	515.9(0.00)	518.0(0.00)	524.6(0.00)				
$\omega_4(a_1)$	666.3(0.02)	678.3(0.02)	668.3(0.02)	626.6(0.00)	642.9(0.01)	629.8(0.00)				
$\omega_5(a_1)$	980.6(1.00)	990.2(0.96)	979.7(1.00)	954.6(0.81)	961.4(0.84)	966.4(0.57)				
$\omega_6(a_1)$	1265.5(0.02)	1272.7(0.02)	1263.7(0.02)	1238.3(0.01)	1246.7(0.01)	1229.0(0.01)				
$\omega_7(a_1)$	1537.3(0.16)	1553.9(0.18)	1534.3(0.15)	1508.1(0.07)	1526.4(0.12)	1498.0(0.01)				
$\omega_8(a_1)$	1617.7(0.95)	1635.0(1.00)	1614.9(0.93)	1586.4(1.00)	1605.9(1.00)	1579.0(1.00)				
$\omega_9(a_1)$	2031.1(0.96)	2079.2(0.73)	2028.4(0.94)	1961.9(0.99)	2018.8(0.82)	1864.1(0.71)				
$\omega_{10}(a_2)$	385.7(0.00)	398.1(0.00)	388.7(0.00)	365.6(0.00)	382.7(0.00)	337.3(0.00)				
$\omega_{11}(a_2)$	564.2(0.00)	598.2(0.00)	567.4(0.00)	529.7(0.00)	562.9(0.00)	524.6(0.00)				
$\omega_{12}(b_1)$	242.1(0.00)	242.0(0.00)	243.4(0.00)	244.8(0.00)	242.8(0.00)	252.8(0.00)				
$\omega_{13}(b_1)$	281.5(0.00)	283.4(0.00)	282.6(0.00)	283.0(0.00)	281.9(0.00)	298.9(0.00)				
$\omega_{14}(b_1)$	584.4(0.04)	595.3(0.03)	586.3(0.04)	540.1(0.06)	562.0(0.04)	503.6(0.05)				
$\omega_{15}(b_1)$	645.9(0.08)	649.0(0.08)	647.4(0.08)	640.6(0.05)	640.6(0.06)	651.6(0.02)				
$\omega_{16}(b_1)$	989.7(0.75)	994.3(0.72)	988.6(0.75)	987.4(0.68)	986.9(0.68)	1020.2(0.58)				
$\omega_{17}(b_1)$	1291.9(0.29)	1295.7(0.27)	1289.0(0.29)	1291.6(0.28)	1298.7(0.30)	1326.5(0.23)				
$\omega_{18}(b_1)$	1412.2(0.02)	1390.4(0.07)	1408.2(0.02)	1443.3(0.02)	1412.1(0.02)	1434.2(0.01)				
$\omega_{19}(b_1)$	1715.0(0.83)	1765.8(0.57)	1712.1(0.81)	1679.9(0.80)	1722.3(0.66)	1653.3(0.64)				
$\omega_{20}(b_2)$	116.7(0.00)	121.0(0.00)	120.6(0.00)	116.4(0.00)	118.7(0.00)	121.8(0.00)				
$\omega_{21}(b_2)$	176.2(0.00)	184.8(0.01)	179.4(0.00)	170.3(0.00)	178.8(0.00)	162.9(0.00)				
$\omega_{22}(b_2)$	431.2(0.00)	444.6(0.00)	434.1(0.00)	424.8(0.00)	436.5(0.00)	381.4(0.04)				
$\omega_{23}(b_2)$	504.5(0.03)	554.1(0.03)	509.1(0.03)	448.1(0.03)	505.7(0.03)	425.3(0.00)				
$\omega_{24}(b_2)$	623.3(0.00)	666.7(0.01)	626.6(0.00)	581.0(0.00)	623.4(0.00)	563.8(0.00)				
									488.2(0.05)	

<sup>a</sup>Computed at the outer minimum-energy structure given in Table IV and described in the text.<sup>b</sup>References 5 and 6.

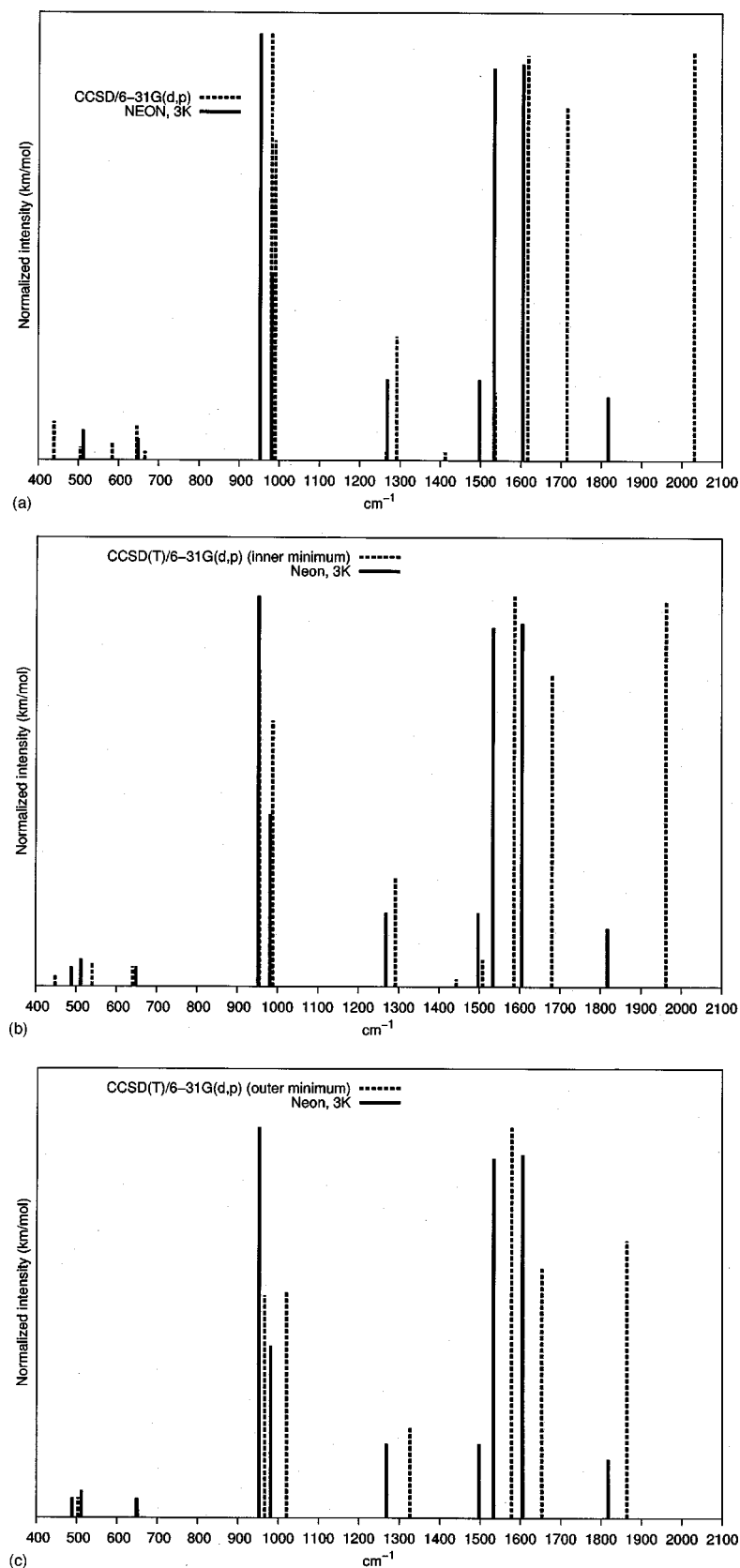


FIG. 5. RHF-CCSD and RHF-CCSD(T) harmonic vibrational spectra for tetrafluoro-*m*-benzyne using a 6-31G(*d,p*) basis. The experimental infrared difference spectrum reported by Wenk and Sander (Refs. 5 and 6) is compared to (a) the CCSD spectrum, (b) the CCSD(T) spectrum for the inner minimum, and (c) the CCSD(T) spectrum for the outer minimum.

In addition, the calculated singlet-triplet (ST) splitting of tetrafluoro-*m*-benzyne is in line with the above description. At CCSD(T)/6-31G(*d,p*), we obtain a value of 26.8 kcal/mol (in favor of the singlet), which is 7 kcal/mol larger than that calculated for *m*-benzyne (20 kcal/mol compared to an experimental value of 21 kcal/mol<sup>57</sup>). An in-

crease in the ST splitting suggests that in the *S* state the single electrons are more strongly coupled either by through-space or through-bond coupling, which in the latter case implies a shorter 1,3-distance.

We note that bicyclic *m*-benzyne structures have also been discussed by Cramer and co-workers<sup>58-60</sup> for various

aza-derivatives of *m*-benzyne, though no experimental evidence is yet available for the molecules investigated.

## V. CONCLUSIONS

The structure of *m*-benzyne was characterized by CCSD, CCSD(T), and CCSDT methods. Basis set effects are small in this case, as indicated by strong similarities in computed geometries with 6-31G(*d,p*) and cc-pVTZ basis sets. However, the level of dynamic electron correlation included in the theoretical model is paramount: while the CCSD methods predicts a bicyclic structure with a C1–C3 distance of 1.56 Å to be the most stable isomer of *m*-benzyne, the CCSD(T) method predicts a monocyclic structure with a C1–C3 distance of approximately 2.1 Å. These results may be understood in terms of three-electron through-bond delocalization effects for which connected triple excitations are essential for a correct description. The best value for distance C1–C3 obtained in this work is 2.013 Å (estimated from the CCSD(T)/cc-pVTZ value of 2.026 and the CCSDT/6-31G(*d,p*) value of 2.093 Å).

Unlike the case of the *p*-benzyne biradical, the choice of reference molecular orbitals has negligible impact on the predicted structure with RHF, UHF, and Brueckner determinants giving essentially identical results, both for the geometry and the vibrational spectrum. The fundamental infrared frequencies calculated for the first time at the CCSD(T) level are in excellent agreement with the measured values and confirm the monocyclic structure of *m*-benzyne. The biradical character of *m*-benzyne is significantly reduced relative to *p*-benzyne because of through-bond coupling leading to a delocalization of the unpaired electrons into the  $\beta$ -position  $\sigma^*(\text{C}-\text{C})$  or the  $\sigma^*(\text{C2}-\text{H7})$  orbitals.

The structure of tetrafluoro-*m*-benzyne, on the other hand, is somewhat more difficult to characterize. At the highest level of theory yet feasible, i.e., CCSD(T)/cc-pVTZ the molecule possesses a flat minimum at a C1–C3 distance of approximately 1.75 Å, which corresponds to weak bonding interaction to give a bicyclic structure. Although C–C bond lengths of that magnitude may no longer be considered to be real bonds, they still involve significant C–C interactions considering the fact that typical transition state distances of breaking such bonds are 2.0–2.2 Å.

The CCSD(T)/6-31G(*d,p*) harmonic vibrational spectrum of tetrafluoro-*m*-benzyne compares reasonably well to the experimental difference spectrum of Wenk and Sander;<sup>5,6</sup> computations with larger basis sets are likely to resolve the remaining discrepancies. There are several features in the measured/calculated infrared spectrum that confirm the computed C1–C3 distance of 1.75 Å.

## ACKNOWLEDGMENTS

This work was supported by a National Science Foundation CAREER award (Grant No. CHE-0133174), a New Faculty Award from the Camille and Henry Dreyfus Foundation, the Jeffress Memorial Trust, and a Lab-Directed Research and Development (LDRD) contract with the U.S. Department of Energy through Sandia National Laboratory (Livermore). DC thanks UOP for a travel grant.

- <sup>1</sup>R. Marquardt, W. Sander, and E. Kraka, *Angew. Chem., Int. Ed. Engl.* **35**, 746 (1996).
- <sup>2</sup>W. Sander, G. Bucher, H. Wandel, E. Kraka, D. Cremer, and W. S. Sheldrick, *J. Am. Chem. Soc.* **119**, 10660 (1997).
- <sup>3</sup>W. Sander, *Acc. Chem. Res.* **32**, 669 (1999).
- <sup>4</sup>W. Sander, M. Exner, M. Winkler, A. Balster, A. Hjerpe, E. Kraka, and D. Cremer, *J. Am. Chem. Soc.* **124**, 13072 (2002).
- <sup>5</sup>H. H. Wenk and W. Sander, *Chem.-Eur. J.* **7**, 1837 (2001).
- <sup>6</sup>H. H. Wenk and W. Sander, *Eur. J. Org. Chem.*, 3927 (2002).
- <sup>7</sup>G. Bucher, W. Sander, E. Kraka, and D. Cremer, *Angew. Chem., Int. Ed. Engl.* **31**, 1230 (1992).
- <sup>8</sup>E. Kraka and D. Cremer, *Chem. Phys. Lett.* **216**, 333 (1993).
- <sup>9</sup>E. Kraka and D. Cremer, *J. Am. Chem. Soc.* **116**, 4929 (1994).
- <sup>10</sup>E. Kraka, D. Cremer, G. Bucher, H. Wandel, and W. Sander, *Chem. Phys. Lett.* **268**, 313 (1997).
- <sup>11</sup>C. J. Cramer, J. J. Nash, R. R. Squires, and W. C. Lineberger, *Chem. Phys. Lett.* **277**, 311 (1997).
- <sup>12</sup>E. Kraka, J. Anglada, A. Hjerpe, M. Filatov, and D. Cremer, *Chem. Phys. Lett.* **348**, 115 (2001).
- <sup>13</sup>M. Winkler and W. Sander, *J. Phys. Chem. A* **105**, 10422 (2001).
- <sup>14</sup>B. A. Hess, *Chem. Phys. Lett.* **352**, 75 (2002).
- <sup>15</sup>L. V. Slipchenko and A. I. Krylov, *J. Chem. Phys.* **117**, 4694 (2002).
- <sup>16</sup>Y. Shao, M. Head-Gordon, and A. I. Krylov, *J. Chem. Phys.* **118**, 4807 (2003).
- <sup>17</sup>P. R. Schreiner, A. Navarro-Vasquez, and M. Prall, *Acc. Chem. Res.* **38**, 29 (2005).
- <sup>18</sup>K. Raghavachari, G. W. Trucks, J. A. Pople, and M. Head-Gordon, *Chem. Phys. Lett.* **157**, 479 (1989).
- <sup>19</sup>P. C. Hariharan and J. A. Pople, *Theor. Chim. Acta* **28**, 213 (1973).
- <sup>20</sup>R. G. Parr and W. Yang, *Density-Functional Theory of Atoms and Molecules* (Oxford University Press, New York, 1989).
- <sup>21</sup>A. D. Becke, *J. Chem. Phys.* **98**, 5648 (1993).
- <sup>22</sup>C. Lee, W. Yang, and R. G. Parr, *Phys. Rev. B* **37**, 785 (1988).
- <sup>23</sup>A. D. Becke, *Phys. Rev. A* **38**, 3098 (1988).
- <sup>24</sup>J. Gräfenstein, E. Kraka, and D. Cremer, *Chem. Phys. Lett.* **288**, 593 (1998).
- <sup>25</sup>J. Gräfenstein and D. Cremer, *Phys. Chem. Chem. Phys.* **2**, 2091 (2000).
- <sup>26</sup>M. Prall, A. Wittkopp, and P. R. Schreiner, *J. Phys. Chem. A* **105**, 9265 (2001).
- <sup>27</sup>J. Gräfenstein, E. Kraka, M. Filatov, and D. Cremer, *Int. J. Mol. Sci.* **3**, 360 (2002).
- <sup>28</sup>V. Polo, E. Kraka, and D. Cremer, *Theor. Chim. Acta* **107**, 291 (2002).
- <sup>29</sup>V. Polo, E. Kraka, and D. Cremer, *Mol. Phys.* **100**, 1771 (2002).
- <sup>30</sup>V. Polo, J. Gräfenstein, E. Kraka, and D. Cremer, *Chem. Phys. Lett.* **352**, 469 (2002).
- <sup>31</sup>D. Cremer, M. Filatov, V. Polo, E. Kraka, and S. Shaik, *Int. J. Mol. Sci.* **3**, 604 (2002).
- <sup>32</sup>T. D. Crawford, E. Kraka, J. F. Stanton, and D. Cremer, *J. Chem. Phys.* **114**, 10638 (2001).
- <sup>33</sup>A. P. Scott and L. Radom, *J. Phys. Chem.* **100**, 16502 (1996).
- <sup>34</sup>R. J. Bartlett, in *Modern Electronic Structure Theory*, Advanced Series in Physical Chemistry Vol. 2, edited by D. R. Yarkony (World Scientific, Singapore, 1995), Chap. 16, pp. 1047–1131.
- <sup>35</sup>T. D. Crawford and H. F. Schaefer, in *Reviews in Computational Chemistry*, edited by K. B. Lipkowitz and D. B. Boyd (VCH, New York, 2000), Vol. 14, Chap. 2, pp. 33–136.
- <sup>36</sup>G. D. Purvis and R. J. Bartlett, *J. Chem. Phys.* **76**, 1910 (1982).
- <sup>37</sup>M. Ritby and R. J. Bartlett, *J. Phys. Chem.* **92**, 3033 (1988).
- <sup>38</sup>R. J. Bartlett, J. D. Watts, S. A. Kucharski, and J. Noga, *Chem. Phys. Lett.* **165**, 513 (1990); **167**, 609(E) (1990).
- <sup>39</sup>M. R. Hoffmann and H. F. Schaefer, *Adv. Quantum Chem.* **18**, 207 (1986).
- <sup>40</sup>J. Noga and R. J. Bartlett, *J. Chem. Phys.* **86**, 7041 (1987); **89**, 3401(E) (1988).
- <sup>41</sup>R. A. Chiles and C. E. Dykstra, *J. Chem. Phys.* **74**, 4544 (1981).
- <sup>42</sup>N. C. Handy, J. A. Pople, M. Head-Gordon, K. Raghavachari, and G. W. Trucks, *Chem. Phys. Lett.* **164**, 185 (1989).
- <sup>43</sup>T. H. Dunning, *J. Chem. Phys.* **90**, 1007 (1989).
- <sup>44</sup>L. Adamowicz, W. D. Laidig, and R. J. Bartlett, *Int. J. Quantum Chem., Quantum Chem. Symp.* **18**, 245 (1984).
- <sup>45</sup>A. C. Scheiner, G. E. Scuseria, J. E. Rice, T. J. Lee, and H. F. Schaefer, *J. Chem. Phys.* **87**, 5361 (1987).
- <sup>46</sup>T. J. Lee and A. P. Rendell, *J. Chem. Phys.* **94**, 6229 (1991).
- <sup>47</sup>G. E. Scuseria, *J. Chem. Phys.* **94**, 442 (1991).

- <sup>48</sup>J. Gauss, W. J. Lauderdale, J. F. Stanton, J. D. Watts, and R. J. Bartlett, *Chem. Phys. Lett.* **182**, 207 (1991).
- <sup>49</sup>J. Gauss and J. F. Stanton, *Chem. Phys. Lett.* **276**, 70 (1997).
- <sup>50</sup>J. F. Stanton and J. Gauss, in *Recent Advances in Coupled-Cluster Methods*, edited by R. J. Bartlett (World Scientific, Singapore, 1997), pp. 49–79.
- <sup>51</sup>P. G. Szalay, J. Gauss, and J. F. Stanton, *Theor. Chim. Acta* **100**, 5 (1998).
- <sup>52</sup>J. F. Stanton, C. L. Lopreore, and J. Gauss, *J. Chem. Phys.* **108**, 7190 (1998).
- <sup>53</sup>J. F. Stanton, J. Gauss, J. D. Watts, W. J. Lauderdale, and R. J. Bartlett, ACESII, 1993. The package also contains modified versions of the MOL-ECULE Gaussian integral program of J. Almlöf and P. R. Taylor, the ABACUS integral derivative program written by T. U. Helgaker, H. J. Aa. Jensen, P. Jørgensen, and P. R. Taylor, and the PROPS property evaluation integral code of P. R. Taylor.
- <sup>54</sup>R. Hoffman, A. Imamura, and W. J. Hehre, *J. Am. Chem. Soc.* **90**, 1499 (1968).
- <sup>55</sup>S. P. de Visser, M. Filatov, P. R. Schreiner, and S. Shaik, *Eur. J. Org. Chem.*, 4199 (2003).
- <sup>56</sup>J. M. Price, K. E. Nizzi, J. L. Campbell, H. I. Kenttämä, M. Seierstad, and C. J. Cramer, *J. Am. Chem. Soc.* **125**, 131 (2003).
- <sup>57</sup>P. G. Wenthold, R. R. Squires, and W. C. Lineberger, *J. Am. Chem. Soc.* **120**, 5279 (1998).
- <sup>58</sup>C. J. Cramer and S. Debbert, *Chem. Phys. Lett.* **287**, 320 (1998).
- <sup>59</sup>W. T. G. Johnson and C. J. Cramer, *J. Phys. Org. Chem.* **14**, 597 (2001).
- <sup>60</sup>W. T. G. Johnson and C. J. Cramer, *J. Am. Chem. Soc.* **123**, 923 (2001).